Adapting Optical-Flow to Measure Object Motion in Reflectance and X-ray Image Sequences

Nancy Cornelius

Department of Electrical Engineering

and

Takeo Kanade

Department of Computer Science

Carnegie-Mellon University
Pittsburgh, Pa. 15213

Abstract

This paper adapts Horn and Schunck's work on optical flow [3] to the problem of determining arbitrary motions of objects from 2-dimensional image sequences. The method allows for gradual changes in the way an object appears in the image sequence, and allows for flow discontinuities at object boundaries. We find velocity fields that give estimates of the velocities of objects in the image plane. These velocities are computed from a series of images using information about the spatial and temporal brightness gradients. A constraint on the smoothness of motion within an object's boundaries is used. The method can be applied to interpretation of both reflectance and x-ray images. Results are shown for models of ellipsoids undergoing expansion, as well as for an x-ray image sequence of a beating heart.

This research was sponsored by the Defense Advanced Research Projects Agency (DOD), ARPA Order No. 3597, monitored by the Air Force Avionics Laboratory Under Contract F33615-81-K-1539.

The views and conclusions contained in this document are those of the authors and should not be interpreted as representing the official policies, either expressed or implied, of the Defense Advanced Research Projects Agency or the US Government.

Introduction

Interpreting the motion of objects from a sequence of images is difficult because image changes may be due to a number of factors. First, image changes may be due to object translations or rotations, or to relative motion of one object such that it occludes another. Second, changes may occur when non-rigid objects change shape or size. Third, parts of an image need not change even though they correspond to a moving object; for example, regions of an image corresponding to flat surfaces of constant reflectance may exhibit no change if the object undergoes only translation. Fourth, changes may result from motion of the observer. Thus, effective algorithms that measure object motion from sequences of images should do two things:

- They should distinguish between image changes due to motion of objects, due to deformation of objects, and due to occlusion.

- They should determine whether regions of an image that exhibit no apparent brightness changes correspond to moving surfaces.

This paper develops methods for assigning velocities to image points by examining changes in brightness at each point in a sequence of images. While many of the techniques may be applicable to environments where the observer is moving, the emphasis will be on interpreting image sequences where the observer is stationary and only objects move. In general, we must notice that motion analysis from images cannot be solved without making assumptions about the underlying motion of objects represented in the image sequence.

Horn and Schunck [3] addressed a problem of computing optical flow from an image sequence. They define optical flow as "the distribution of apparent velocities of movement of brightness patterns" in a sequence of images. Usually optical flow refers to the flow of the imaged world across the retina as a biological observer moves continuously through the world. However, if we assume a stationary viewer and assume there are no changes in the brightness patterns as a result of the motion, then Horn and Schunck's definition of optical flow gives the velocities of objects projected onto the image plane. To say that there are no changes in the brightness patterns means that the image brightness corresponding to a single physical point on an object is the same from one frame to the next. This restriction permits only translation of objects parallel to the image plane and does not allow arbitrary rotations or perspective transformations. In order to compute optical flow, Horn and Schunck assumed that the velocities varied smoothly over the entire image. This assumption has limited utility in real images where object boundaries are usually places of discontinuous velocity for both the case of a moving object and for an observer moving with respect to a static scene.

Our approach also involves computing velocities at the points in an image, but our method differs from Horn and Schunck's in two important ways. First, the the velocity smoothness constraints are applied only within regions that are separated from the rest of the image by recognizable boundaries. Velocities are free to change abruptly across these boundaries. Second, changes in the brightness patterns are allowed so that velocities more closely represent the arbitrary motions of objects projected onto the image plane. For example, gradual shading changes that occur with rotation relative to the light source may be accommodated.

The methods developed are applied to models of ellipsoids undergoing expansion and to x-ray image sequences of a beating heart. In the latter case the pattern changes of interest are those that occur when the heart changes shape in a direction perpendicular to the image plane.

Problem Statement

If there is no a priori knowledge about the structure of objects in a scene, then measurement of velocity relies on local information about temporal and spatial gradients of image brightness. This local information provides only one constraint, the change in brightness at a given point, while the velocity of a point in an image has two components. In simple situations, where moving objects only undergo translation parallel to the image plane without changing their pattern in the image, this constraint determines the component of velocity parallel to the brightness gradient. When the brightness gradient is zero in the direction of motion (eg. flat region of an object with constant reflectance or a stripe pattern in the direction of motion), then there is no local velocity information. In all cases additional constraints must be imposed to determine the two components of velocity in the image plane as well as to determine the changes in the image pattern.

Let the image brightness projected by a point on a moving object at a time t be given by $I(x,y,t)$. At a later time $t+dt$ the same object point has moved so that its projected position in the image plane is given by $(x+dx,y+dy)$. The brightness of this point may have changed to a value $I(x+dx,y+dy,t+dt)$. Such a change occurs when lighting and shading change as an object rotates or when the object itself changes shape. The total rate of change of brightness dI/dt is given by:

$$\frac{dI}{dt} = \frac{\partial I}{\partial x}\frac{dx}{dt} + \frac{\partial I}{\partial y}\frac{dy}{dt} + \frac{\partial I}{\partial t} \tag{1}$$

where $\partial I/\partial x$ and $\partial I/\partial y$ are the x and y components of the spatial brightness gradient and $\partial I/\partial t$ is the temporal brightness change measured at the point (x,y). The three variables that are to be determined are the x and y components of velocity, i.e. dx/dt and dy/dt, respectively, and the brightness change dI/dt. To simplify the notation, we introduce the abbreviations I_x, I_y and I_t for the partial derivatives of brightness with respect to x, y and t and the abbreviations v_x and v_y for the x and y velocity components. Equation (1) can then be rewritten in the following way:

$$\frac{dI}{dt} = I_x v_x + I_y v_y + I_t \tag{2}$$

To solve this equation for the velocities (v_x, v_y) and the rate of brightness change (dI/dt), other constraints must be applied that restrict the allowable motions. For example, the assumption can be made that the velocity and pattern changes are constant or that they change smoothly within a region. It could also be assumed that the velocities and patterns vary in a constrained manner over time [4].

In the next section, we review Horn and Schunck's method for computing optical flow, and identify problems with it. The remaining sections propose a set of modifications and extensions to cope with those problems. First, we present a technique that permits velocity flow discontinuities at boundaries. Then we suggest a way to accommodate some of the changes in brightness patterns that occur as a result of motion. The final section presents results obtained by applying the modifications to a model of an expanding ellipsoid and an example that incorporates all of these techniques to analyze heart motion from a sequence of x-ray images.

Horn and Schunck's Method for Computing Optical Flow

Horn and Schunck [3] assumed no pattern change in the image so that the brightness change with time corresponding to a single physical point dI/dt is equal to zero, i.e.:

$$I_x v_x + I_y v_y + I_t = 0 \tag{3}$$

This assumption severely limits the allowable motions. Rotations, translations in depth and deformations often result in changes in the image brightness pattern and violate this assumption. Horn and Schunck made the additional assumption that neighboring points have similar velocities. To implement this smoothness constraint, they constrained the local change in velocity by minimizing the square of the magnitude of the spatial gradient of the velocity components:

$$\varepsilon^2 = \left(\frac{\partial v_x}{\partial x}\right)^2 + \left(\frac{\partial v_x}{\partial y}\right)^2 + \left(\frac{\partial v_y}{\partial x}\right)^2 + \left(\frac{\partial v_y}{\partial y}\right)^2 \tag{4}$$

In order to solve for the optical flow v_x and v_y, Horn and Schunck combined the two assumptions (the zero brightness change and the smoothness constraint) by minimizing the following function:

$$\int \left[\left(\frac{dI}{dt}\right)^2 + \alpha^2(\varepsilon^2)\right] dxdy \tag{5}$$

where the integral is over the entire image and α^2 is a weighting factor that depends on the noise in the gradient measurements. The following iterative formulae provide the solution for the flow velocities that minimizes equation (5):

$$v_x^{k+1} = \bar{v}_x^{k} - \frac{I_x(I_x\bar{v}_x^{k} + I_y\bar{v}_y^{k} + I_t)}{\alpha^2 + I_x^2 + I_y^2} \tag{6}$$

$$v_y^{k+1} = \bar{v}_y^{k} - \frac{I_y(I_x\bar{v}_x^{k} + I_y\bar{v}_y^{k} + I_t)}{\alpha^2 + I_x^2 + I_y^2}$$

where $\bar{v}_x^{k}$ and $\bar{v}_y^{k}$ denote local averages of the velocity components computed at the kth iteration. A region where there is no apparent local velocity information (eg. flat region of constant reflectance) will derive its velocity from the surrounding region, because during the iterative process, velocities will tend to propagate and fill in these regions.

There are three primary problems with this technique. The first two involve the boundaries. First, the technique does poorly when there are discontinuities in the velocity field or in the brightness gradients, because of the smoothness assumption. The discontinuities occur at object boundaries. Second, the same property that allows velocities to propagate within an object tends to extend erroneous velocities outside the area of an object. The problem is most conspicuous for the case where an object is moving against a uniform background. In this case it is not possible to distinguish the velocity of the object from the velocity assigned to the uniform background. Third, motion is constrained to be parallel to the image plane because of the assumption that an object does not change the way it appears in the image from frame to frame.

Boundary Constraints

The previous section suggests that discontinuities in velocity which occur at object boundaries must be explicitly accounted for in order to accurately determine velocities within the boundaries. We propose to allow for these discontinuities by applying the smoothness constraint separately to regions on either side of an image boundary. This can be done once the projection of the object boundaries have been located in the image. As we see next, implementation does not require that the image be segmented into regions corresponding to objects, rather only that the location of *possible* object boundaries be determined.

Image boundaries occur when one object moves in front of another: these are called occluding boundaries. Image boundaries can also occur due to the painted patterns or non-occluding edges on the object: these are non-occluding boundaries. (There are also boundaries due to object shadows, but these are not explicitly dealt with here.) In terms of motions across them, there is an important difference between occluding and non-occluding boundaries. A non-occluding boundary has consistent motion on both sides -- there is no velocity discontinuity. The regions on both sides of an occluding boundary can have different velocities. We must process velocity flow data at a boundary differently according to the type of boundary. The smoothness constraint is enforced across non-occluding boundaries, but not across occluding boundaries. This procedure permits spatial discontinuities in flow velocity to occur when one object moves in front of another.

To apply this method, we need not predetermine whether a boundary is occluding or non-occluding. First, the nearby velocities are computed based on an assumption of non-occlusion; the smoothness constraint is applied across the boundary. Next, the velocities are recalculated assuming occlusion; the smoothness constraint is not enforced across the boundary. Finally, the result that best satisfies the equation for dI/dt (equation (2)) and the smoothness constraint is retained. In this way, the boundary types can be locally determined without explicit segmentation of the image into object regions. This test is repeated with each iteration.

Pattern Changes

A pattern change refers to the change in image brightness of the same physical point on an object from one frame to the next. A pattern change will occur when points on the object are obscured or revealed in successive image frames. This type of change causes discontinuities in the velocity across occluding boundaries. These changes have been accommodated by the method in a previous section.

There is also another type of pattern change. For example, when an object rotates and the lighting hits the object in a different way, it results in different shading. For a Lambertian surface the shading change of a given physical point on an object is given by:

$$\frac{dI}{dt} = \frac{d}{dt}(k \cos(\tau)) = -k \sin(\tau)\frac{d\tau}{dt} \tag{7}$$

where τ is the angle between the incident light and the the surface normal, and k is a constant. If the surface orientation is known, then dI/dt gives a measure of the change in orientation.

Here we propose to allow for such pattern changes in the image by constraining them to vary smoothly within boundaries. We can think of the pattern change (dI/dt) as another velocity component. While dI/dt is not strictly a velocity, we constrain the variations in dI/dt to vary smoothly within object boundaries, just as was done for the velocity components. Thus we can define a smoothness measure of change in brightness variation:

$$\varepsilon_B^2 = \left[\frac{\partial}{\partial x}\left(\frac{dI}{dt}\right)\right]^2 + \left[\frac{\partial}{\partial y}\left(\frac{dI}{dt}\right)\right]^2 \tag{8}$$

New Algorithm

Now we can present our new algorithm which incorporates the considerations on boundaries and pattern changes. To summarize, this algorithm assumes: (a) the brightness changes of a single physical point can be described by the first order expansion, equation (2); (b) velocity changes in a neighborhood are similar, unless the neighborhood contains an occluding boundary; (c) the rate of pattern change (*dI/dt*) is also similar in a neighborhood. To impose these assumptions we define an error factor for each.

The first factor is the error in satisfying equation (2), i.e.:

$$\varepsilon_I^2 = \left(\frac{dI}{dt} - I_x v_x - I_y v_y - I_t\right)^2 \tag{9}$$

Since we allow *dI/dt* to be nonzero, it is included in ε_I^2. The second error factor is a measure of the departure from a spatially smooth velocity field, ε_S^2, which is the same as equation (4). The third error factor is given by equation(8) and measures the departure from a spatially smooth pattern change.

We minimize the sum of these error factors computed over the image:

$$\text{minimize} \sum_i \sum_j \varepsilon_I^2(i,j) + \alpha^2 \varepsilon_S^2(i,j) + \beta^2 \varepsilon_B^2(i,j) \tag{10}$$

An iterative form of the solution is found for the velocities at the *(k+1)* iteration in terms of the spatial and temporal brightness gradients and the neighboring velocities at the *k-th* iteration:

$$v_x^{k+1} = \bar{v}_x^k - \frac{\beta^2 I_x\left[I_x \bar{v}_x^k + I_y \bar{v}_y^k + I_t - (\overline{dI/dt})^k\right]}{\alpha^2 + 2\alpha^4\beta^2 + \alpha^2\beta^2 I_x^2 + \alpha^2\beta^2 I_y^2} \tag{11}$$

$$v_y^{k+1} = \bar{v}_y^k - \frac{\beta^2 I_y\left[I_x \bar{v}_x^k + I_y \bar{v}_y^k + I_t - (\overline{dI/dt})^k\right]}{\alpha^2 + 2\alpha^4\beta^2 + \alpha^2\beta^2 I_x^2 + \alpha^2\beta^2 I_y^2}$$

$$\left(\frac{dI}{dt}\right)^{k+1} = \left(\overline{\frac{dI}{dt}}\right)^k + \frac{\left[I_x \bar{v}_x^k + I_y \bar{v}_y^k + I_t - (\overline{dI/dt})^k\right]}{\alpha^2 + 2\alpha^4\beta^2 + \alpha^2\beta^2 I_x^2 + \alpha^2\beta^2 I_y^2}$$

where $\bar{v}_x^k$ and $\bar{v}_y^k$ denote averages of the neighboring velocities at the *k-th* iteration and $(\overline{dI/dt})^k$ denotes the average pattern change at the *k-th* iteration. This iterative procedure is applied everywhere in the image, but points in the neighborhood of a boundary are treated differently. Boundaries are located by finding zero crossings in the Laplacian of brightness [1] in each of a sequential pair of images and forming a union of such zero crossings. The size of a neighborhood is determined by the size of the region over which

the smoothness constraint ϵ_S^2 is computed. Velocities are computed separately using points in the neighborhood on one side of the boundary and again using points in the neighborhood that span the boundary. This yields two different estimates for the velocity. The estimate that minimizes $\epsilon_I^2 + \alpha^2 \epsilon_S^2 + \beta^2 \epsilon_B^2$ is used.

Results

Model of Expanding Ellipsoid

The algorithm described in this paper was tested with a sequence of images generated by modelling an ellipsoid that expands uniformly in all directions. The ellipsoid is assumed to have Lambertian surface properties and to be illuminated with a distant source perpendicular to the image plane. The image is resolved to 64 by 64 pixels and quantized to 256 brightness levels (see Figure 1A). The maximum velocity of any point in the image is approximately 0.5 pixels per frame. The background is uniform and therefore provides no information about motion. The actual velocity vectors for the expanding ellipsoid are shown in Figure 1B. These are the results we would like to obtain using our algorithm.

Figure 2 shows the results of applying Horn and Schunck's optical flow technique (equation 6) to the expanding ellipsoid. Here the smoothness constraint is applied across object boundaries. While the velocities are determined fairly accurately within the object, they are propagated erroneously beyond the object boundaries. The total error over the entire image is approximately 15%. When velocity discontinuities are taken into account as outlined above, a more accurate estimate of velocities is obtained as in Figure 3. We see that use of boundary information results in a clear demarcation of velocities within and without the object. The residual errors do not extend substantially beyond the boundaries of the object. The total error is 5%. However, the algorithm tends to overestimate the actual velocities in the vicinity of the boundary. Such inaccuracies are expected, because of the discontinuities in the brightness gradient that occur at the border between one object and another. One way to avoid this problem and possibly improve the flow velocity estimates throughout a region is to determine velocities at the boundaries of the region using another technique (see for example [2]). Such velocities at the boundary provides intitial conditions and remain fixed in the iterative procedure. To see this effect, the actual velocities at the boundary were supplied as initial conditions and remained fixed for the iterative procedure. The result is shown in Figure 4. The total error is less than 3%. For the case of the expanding ellipsoid, the velocities inside the boundary region were close to the correct values whether or not the initial boundary velocities were specified. However, there are probably other cases when a good initial guess of velocity at the boundary will substantially improve the velocity estimates inside the bounded region.

Application to X-ray Images

Though these techniques have been developed for objects imaged in visible light, we have begun to explore application of these techniques to x-ray images. Our goal is to use them to analyze motion of the heart from cine angiograms.

When optical flow techniques are applied to x-ray images, the results have a different meaning. At each point in an x-ray image, the brightness depends on the amount and density of the mass between the x-ray source and the film. Because brightnesses depend on object densities instead of reflectance, the velocities found by this method no longer apply to single physical points on the surfaces of objects. For simplicity, we assume that the density does not change in time and that the brightness changes therefore represent depth changes. In angiograms where radio-opaque dye is injected into the bloodstream, the primary x-ray

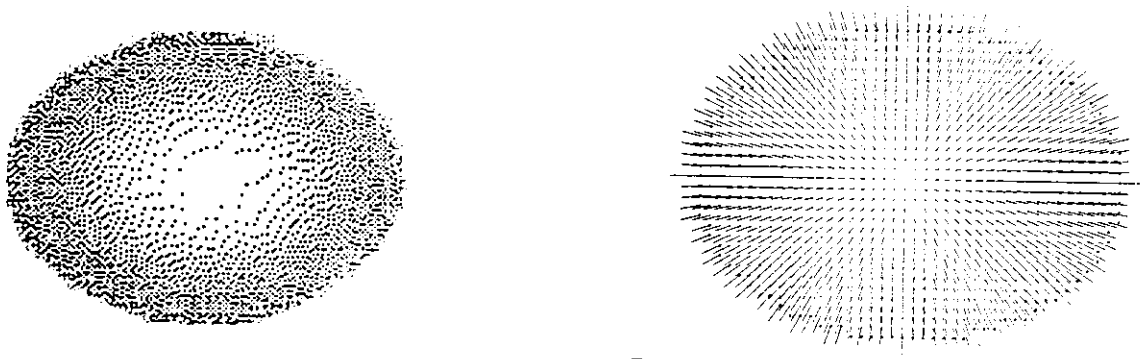

Figure 1: An image sequence was obtained by modelling an ellipsoid that expands uniformly in all directions. One frame of the sequence is shown in (A). At each point in the image we have computed the magnitude and direction of the local image velocity. The velocity vectors at each point in the image are plotted here as short line segments representing magnitude and direction. The correct velocity flow pattern determined from the model is shown in (B).

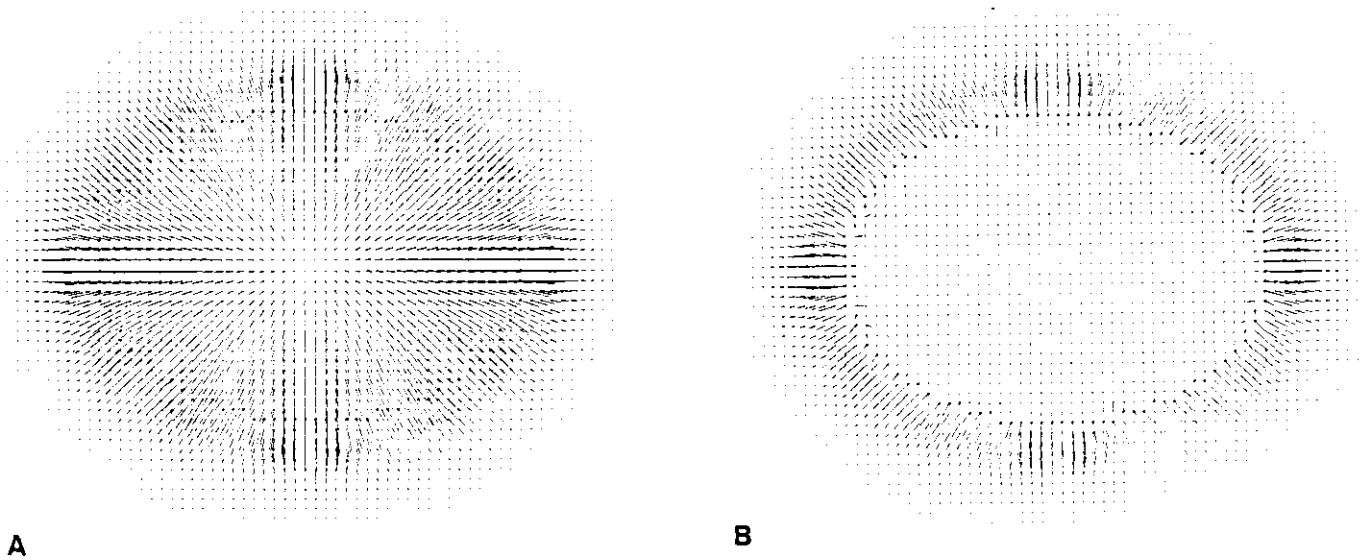

Figure 2: The velocity vectors for the expanding ellipsoid were calculated using Horn and Schunck's optical flow algorithm. The resulting flow pattern is shown in (A). No boundary constraints were imposed, so that the velocity smoothness constraint was applied across the boundaries. The result is that the velocities propagated outside the boundary. A vector plot of the velocity errors is shown in (B). Initial velocities were set to zero. The results are shown after thirty-two iterations.

attenuators are the dye and calcified bone. For this case, the assumption that pattern changes reflect changes in the depth of the heart is accurate since the dye filled heart is the primary source of motion.

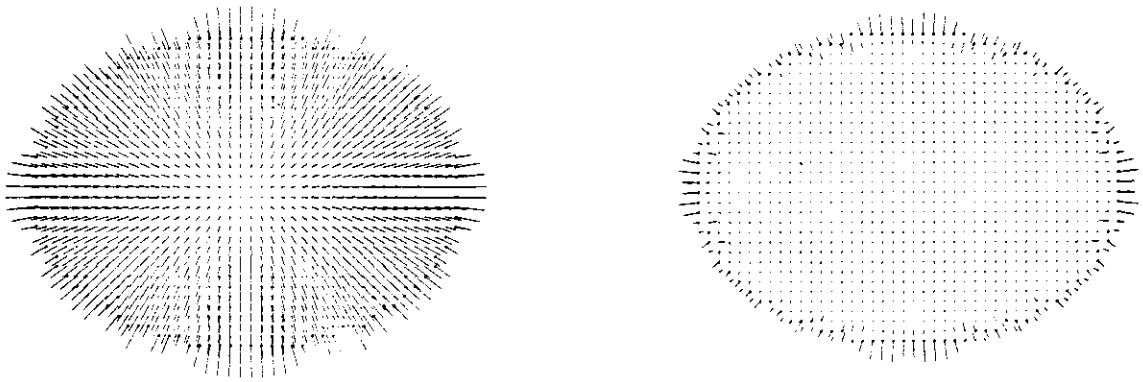

Figure 3: The velocity flow pattern in (A) was calculated for the expanding ellipsoid assuming that flow discontinuities could occur at the boundaries. The boundaries used are indicated by heavy black dots at the base of some of the velocity vectors. Velocity errors are shown in (B). The velocities computed at the boundaries are substantially greater than the actual velocities, however, the velocities inside the ellipsoid are very close to the actual velocities. Again, the initial velocities were set to zero and the results are shown after thirty-two iterations.

X-ray images have two advantages over reflectance images of opaque objects. First, depth information is available. Second, objects are not totally occluded. The disadvantage is that a point in the image does not generally correspond to a single point on a single object. Thus the flow velocities take on a different meaning for x-ray images, as described above. To understand what this difference means, consider a reflectance image and an x-ray density image of the same object, an expanding sphere. (See Fig. 5.) In the reflectance image the brightness due to a single physical point on the sphere is the same in successive images, because it has the same surface orientation. Therefore, to determine velocity at a given point, we need only find a point of matching brightness that satisfies the global smoothness constraint. If we look at brightness along one dimension of the image, then the velocities are found by matching points of similar brightness in successive frames. (See Figure 5A.)

In an x-ray density image which records the z height as the brightness, such a simple matching of similar brightnesses frequently does not yield sensible velocities. In fact, there may be many points in one image for which there is no matching brightness in successive images. As shown in Figure 5B, matching points in successive frames of the x-ray image of a sphere based on similar brightness values, yields very large velocities near the densest part of the imaged sphere (i.e. center) where the actual velocities are small. A meaningful description of the motion from the density image would be obtained by taking the rate of brightness change (dI/dt) into account. This can be interpreted as a change in depth perpendicular to the image plane. (See Figure 5C.) For x-ray images of a beating heart, the brightness at a point in the image is dependent on the depth of the heart cavity perpendicular to the image plane. Thus the pattern changes will reflect the expansion or contraction movement of the heart in the direction perpendicular to the image plane.

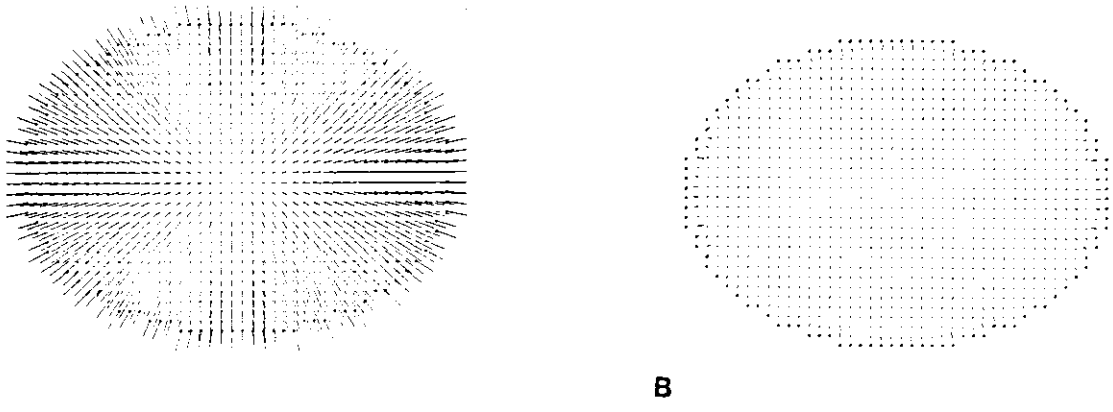

Figure 4: The velocity flow pattern in (A) was calculated for the expanding ellipsoid with the velocities at the boundaries set to the actual values. As in Figure 3, discontinuities in velocity flow were permitted at the boundary. The boundaries used are indicated by heavy black dots. The plot in (B) shows the velocity errors. The total error is less than 3% after thirty-two iterations.

Model of X-ray Image of Expanding Ellipsoid

We show an example for a sequence of images generated by modelling an ellipsoid that expands with time. The brightness is proportional to the depth of the ellipsoid perpendicular to the image plane. The ellipsoid is expanding in all directions so that the size and brightness change as a function of time. The velocities projected on the image plane are the same as for the case of the reflectance image. We expect the brightness changes to be proportional to the actual brightness or depth. Figure 6 shows these anticipated velocities and brightness changes. Figure 7 shows the velocity field which is computed by the Horn and Schunck method (i.e., with the assumption that there are no pattern changes, $dI/dt=0$). As expected, we obtain a large flow discontinuity at the center of the image of the ellipsoid. Figure 8 shows the result of our method in which pattern changes are allowed. The velocities and pattern changes are very close to the expected results.

Experimental Results for Heart Images

We have applied the methods described in this paper to x-ray images of a dog's heart taken on film at 60 frames a second. Figure 9 shows an example of a single frame of the cine angiogram. A radio-opaque dye was injected into the pulmonary artery just before the image sequence was taken. The dye can be seen filling the left ventricle, the aorta and some of the coronary arteries. The other obvious structures in the images are a couple of catheters left over from some previous injections. The film was digitized with 8 bits per pixel and resolved to 100 x 100 pixels.

The velocities were computed using equations (11). Pattern changes caused by the expansion and contraction of the heart perpendicular to the image plane were permitted and discontinuities in the velocity flow were accommodated at image boundaries as described above. The image boundaries were located at the

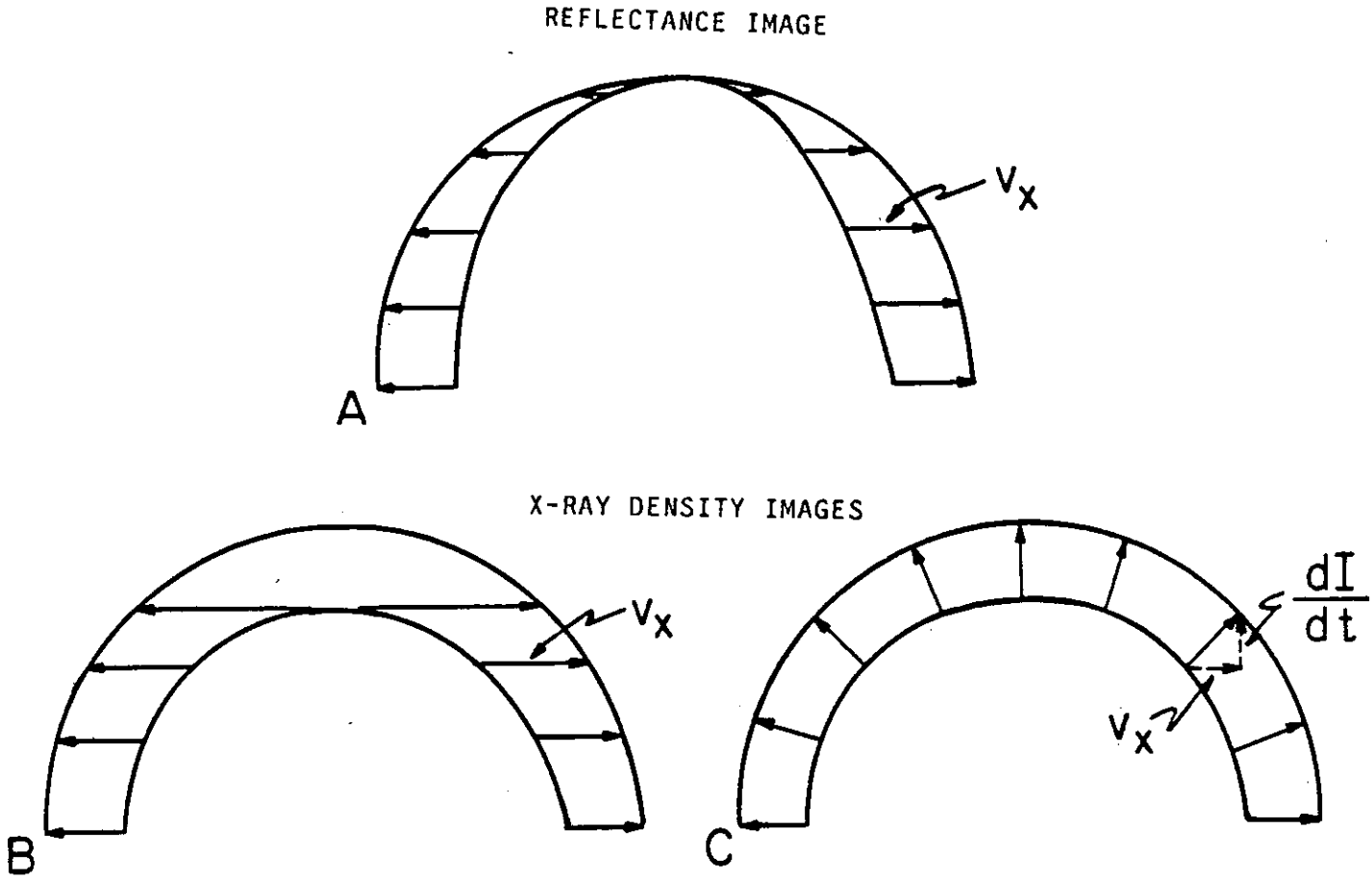

Figure 5: When a sphere expands in a reflectance image, the profile of brightnesses in a cross-section parallel to the x-axis changes as shown in (A). We assume a distant light source perpendicular to the image plane. The brightness of points on the surface do not change as the sphere expands, so surface motion can be measured by matching points of similar brightness that satisfy the smoothness constraint. When a sphere expands in an x-ray density image, the brightness of each surface point increases as shown in (B) and (C). It is no longer possible to determine velocities by matching brightnesses. We expect the velocities to be the same as for the reflectance case. However, if we simply match brightnesses as in (B),we obtain very large velocities near the center of the imaged sphere where we expect very small velocities, as well as a large flow discontinuity at the center of the sphere. If, as in (C), we allow for smoothly varying brightness changes (dI/dt) in addition to the motion in the plane parallel to the image, then velocities in the image plane are as expected.

zero crossings of the Laplacian of a smoothed version of a pair of sequential images. The computed velocities are shown in Figure 10. To verify these results, the computed motion description is used to predict the brightness in a subsequent image from the brightness in the previous image. A comparison of the predicted and actual images shows an error of less than 0.5%. While this does not show that the motion description is actually a good one, it does show that the algorithm is working as expected. In order to get a subjective opinion of the validity of the motion description, we have generated a movie of the velocity vectors for an entire heart cycle and shown that it coincides well with the apparent motion seen in the actual cine angiogram. While the motion description obtained from the analysis of x-ray images may be useful, it does not provide explicit information about motion of object surfaces. This sort of information might be obtained by using additional views of the object from different angles, or by considering a priori information about the object's shape or symmetry.

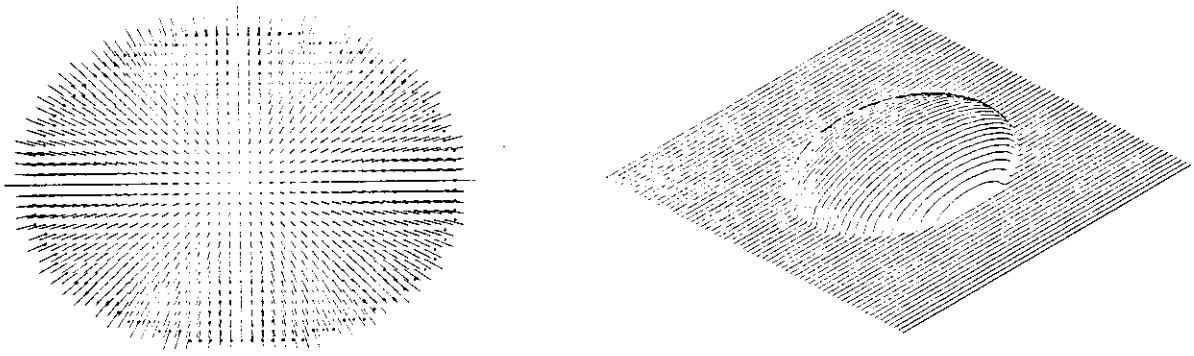

A B

Figure 6: The expanding ellipsoid was modelled again, but the brightness at each point in the image now corresponds to the depth of the ellipsoid measured perpendicular to the image plane. The result is similar to an x-ray image of an ellipsoid. The velocities calculated from the model are shown in (A) and the rate of pattern change (dI/dt) is shown in (B). The pattern changes can be thought of as changes in depth.

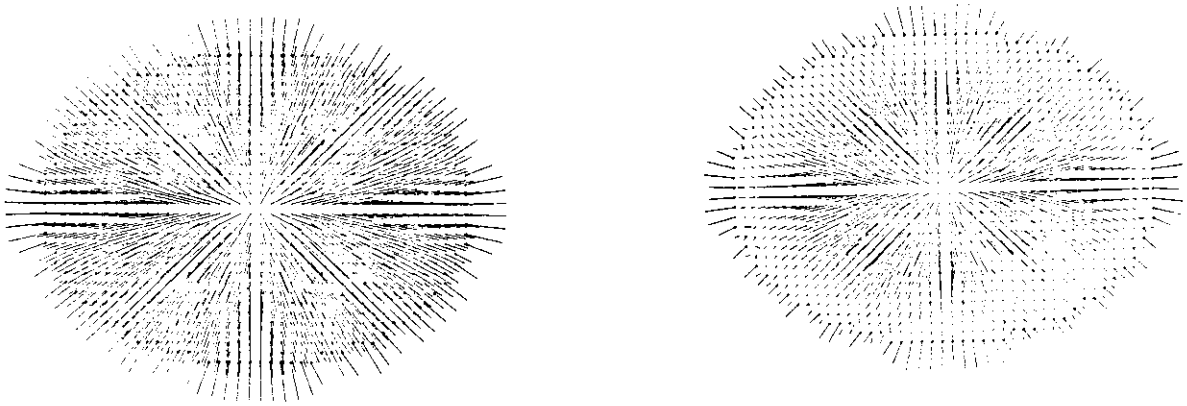

A B

Figure 7: (A) The computed velocities for density images of the expanding ellipsoid assuming no pattern changes, i.e., $dI/dt=0$. Note the large discontinuity in velocity flow at the center of the imaged ellipsoid and the very large velocities near the center. (B) The errors in the computed velocities. Results are shown after 32 iterations.

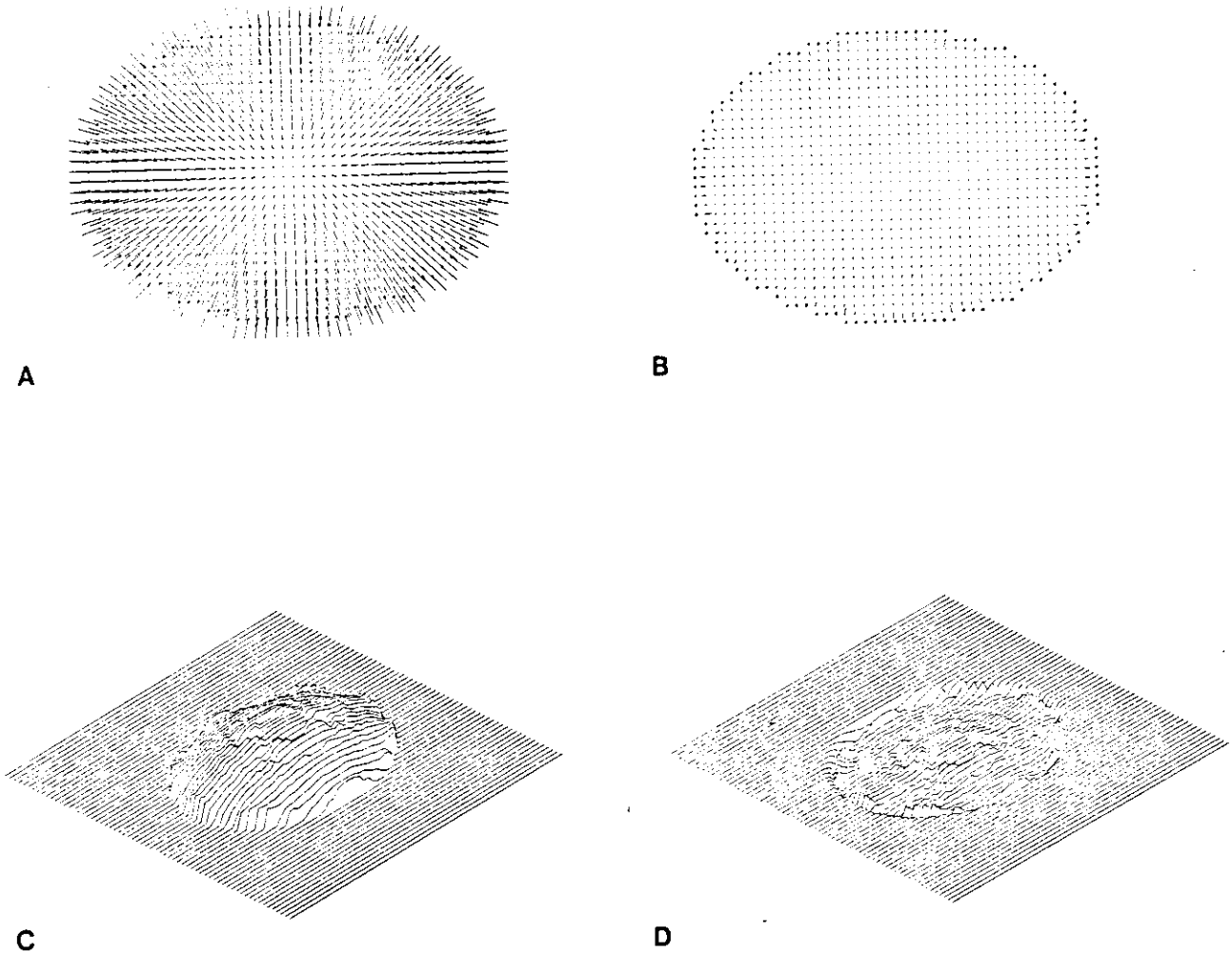

Figure 8: The velocities were computed for density images of the expanding ellipsoid allowing for velocity discontinuities at boundaries and allowing for pattern changes. The velocities were preset to the actual values at the boundaries. All other velocities were initialized to zero. The boundaries used are indicated by heavy black dots. Results are shown after 32 iterations. (A) The velocity flow pattern computed for the image plane. (B) The velocity errors in (A). (C) The computed pattern changes or depth changes. (D) The errors in (C).

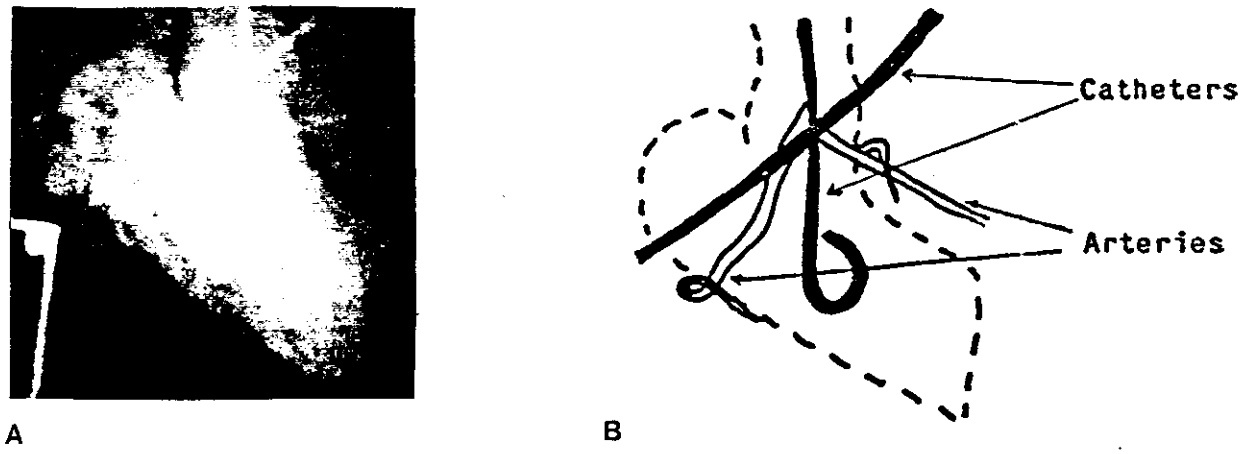

Figure 9: Experimental results were obtained for a sequence of x-ray images of a dog's heart injected with radio-opaque dye. (A) An example of a single frame in the sequence. (B) A line drawing identifying the structures.

Summary

This paper extends the work of Horn and Schunck on optical flow. Their velocity smoothness constraint is relaxed at boundaries to permit discontinuities in estimated velocity where there are occluding boundaries. It is not necessary to segment the image into objects in order to use boundary information. Rather it is only necessary to locate possible boundaries which can be done by locating zero crossings in the Laplacian of the smoothed image brightness. Images of an expanding ellipsoid were used to test the resulting iterative algorithm. The results showed that discontinuities in the velocity flow could be accommodated, but that the velocity at the actual boundary may be inaccurate. It is possible to estimate the velocities at the boundary using another technique and then to use these estimates as input to the iterative algorithm.

Though the techniques were originally developed for reflectance images, we have begun to apply them to x-ray density images. To do this it has been necessary to relax Horn and Schunck's restriction that the appearance of an object not change from one image to the next. This was done by assuming that the pattern changes in the image vary gradually within object boundaries. Velocity flow patterns for x-ray images of the expanding ellipsoid were obtained in this way. The results showed that the computed velocities parallel to the image plane were very close to those obtained for reflectance images and the pattern changes were very nearly proportional to the velocities perpendicular to the image plane. The technique was also used to analyze x-ray cine angiograms of a beating heart and produced a subjectively good description of the motion.

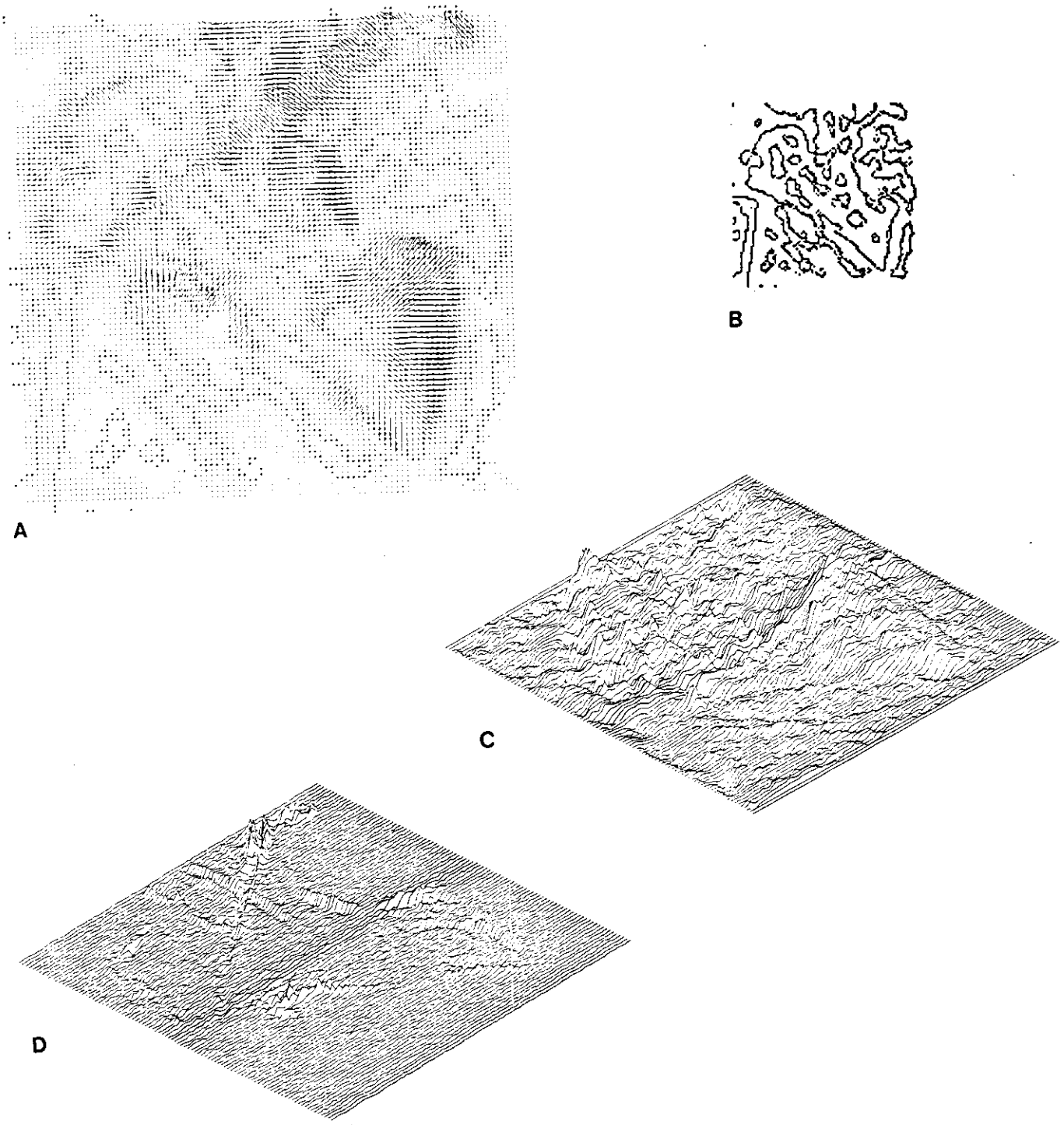

Figure 10: A sequence of x-ray images of a dog's heart were processed to obtain velocity information. Velocity discontinuities were permitted at image boundaries. (A) The velocity flow vectors. The boundaries used are indicated by heavy black dots in the figure. (B) The boundaries alone. (C) The depth changes or pattern changes. (D) The error in predicting the subsequent frame from the previous frame given the motion description in (A) and (C). The total error is less that 0.5%. Initial velocities were set to zero. The results are shown after twenty iterations.

Acknowledgements

We would like to thank Bob Selzer and the Biomedical Imaging Lab at the Jet Propulsion Labs in Pasadena, California for providing us with the digitized cine angiogram data.

References

[1] Hildreth, Ellen C.
Implementation of a Theory of Edge Detection.
Technical Report AI-TR-579, Artificial Intelligence Laboratory, MIT, April, 1980.

[2] Hildreth, Ellen C.
The Integration of Motion Information Along Contours.
In *Proceedings of the Workshop on Computer Vision Representation and Control*, pages 83-91. IEEE, August, 1982.

[3] Horn, Berthold B. K. and Schunck, Brian G.
Determining Optical Flow.
Artificial Intelligence 17:185-203, 1981.

[4] Yachida, Nasahiko.
Determining Velocity Map by 3-D Iterative Estimation.
In *Proceedings of Seventh IJCAI*, pages 716-718. Vancouver, B.C., Canada, August, 1981.